ChemComm

Programmable RNA methylation and demethylation using PUF RNA binding proteins

Journal:	*ChemComm*
Manuscript ID	CC-COM-11-2019-009298.R1
Article Type:	Communication

COMMUNICATION

Programmable RNA methylation and demethylation using PUF RNA binding proteins

Received 00th January 20xx,
Accepted 00th January 20xx

DOI: 10.1039/x0xx00000x

Kouki Shinoda, [a] Akiyo Suda, [a] Kenko Otonari, [a] Shiroh Futaki [a] and Miki Imanishi *[a]

New methods to control local RNA methylation are needed to elucidate the function of individual m6A. Here, fusion proteins between the programmable RNA binding protein PUF and the m^{6}A demethylase FTO or METTL14 methyltransferase were designed. FTO-PUFs and METTL14-PUFs showed sequence-specific RNA demethylation and methylation activities, respectively.

The methylation of adenosines at the N6 position (m^{6}A) is the most abundant mRNA modification, regulating various aspects of mRNA metabolism, such as mRNA stability, localization, and translation, ultimately controlling gene expression. Two m^{6}A writers, the Methyltransferase-like 3 and 14 (METTL3 and METTL14) form an obligate heterodimer and "write" the *N*^{6}-adenosine methyl on the central adenosine in the RRACH (R: A, G; H: A, C, U) consensus sequences[1]. Fat mass and obesity-associated protein (FTO) or alpha-ketoglutarate-dependent dioxigenase alkB homolog 5 (ALKBH5) catalyze the demethylation reaction and are called "erasers"[2, 3]. So far, the importance of m^{6}A RNA methylation in various biological processes including differentiation[4, 5], tumorigenesis[6, 7], circadian clock[8], and virus infection[9] has been shown through knockdown or overexpression of these m^{6}A regulatory enzymes or by using small molecules to change methylation levels. However, the specific functions of a given m^{6}A site can only be speculated from such large-scale interventions, since methylated nucleotides throughout the transcriptome will be affected, causing many secondary effects. New methods that enable mRNA methylation states to be tuned at specific sites, hence in a sequence-specific manner, are required.

To target a specific mRNA site to achieve programmable post-transcriptional regulation, CRISPR-based RNA-targeting technologies and modular RNA-binding proteins have been developed[10-12]. Here, we harnessed the mRNA-sequence specificity of the modular RNA-binding proteins Pumilio and FBF homology protein (PUF). The mRNA binding region of PUFs consists of eight structural repeats, each containing ~36 amino acids, flanked by N- and C-terminal repeats (Fig. S1A)[13, 14]. Each of these eight PUF repeats recognizes a single nucleotide using three amino acid residues at specific positions. By substituting the amino acids in the repeats, mutant proteins have been created targeting various mRNA sequences of eight bases[15-19]. In addition, artificially designed multiple-repeats PUFs were shown to bind to longer mRNA sequences, which made it possible to target a specific RNA sequence in the transcriptome[15, 20-22]. So far, PUF proteins have been fused with various effector domains for splicing[23], translational control[19, 24-26], cleavage of mitochondrial-encoded gene transcripts[27], or visualization of endogenous mRNAs[28-32]. Considering such achievements, PUF would be a useful guide to target m^{6}A-regulatory enzymes to a specific locus and manipulate RNA methylation status. In this study, we demonstrate the feasibility of this approach by genetically engineering a fusion between FTO or METTL14 with the customizable RNA binding protein PUF (Scheme 1).

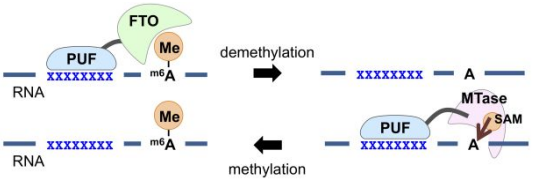

Scheme 1 Concept of the targeted demethylation and methylation. FTO or METTL14 was genetically fused with a designable RNA binding protein, PUF. The fusion proteins are expected to control RNA (de)methylation close to the PUF binding site.

To demethylate target m^{6}A sites, FTO-PUF**a** was constructed, in which the RNA binding domain of Pumillio 1 (PUM1, here denoted as PUF**a**), recognizing 5'-UGUAUAUA-3'[16, 17], was fused with FTO using a $(GSS)_2$ flexible linker (Scheme 1, upper). The fusion protein was expressed in *E. coli*, and purified and used for *in vitro* demethylation assay. RNA demethylation by FTO or FTO-PUF**a** was evaluated by the MazF cleavage assay which we have developed recently (Fig. S1B)[33], based on the *E. coli* MazF, a 5'-ACA-3' specific

[a] *Institute for Chemical Research, Kyoto University, Uji, Kyoto 611-0011, Japan. E-mail: imiki@scl.kyoto-u.ac.jp.*
Electronic Supplementary Information (ESI) available: [details of any supplementary information available should be included here]. See DOI: 10.1039/x0xx00000x

endoribonuclease, which is unable to cleave the methylated 5′-m^{6}ACA-3′ (Fig. 1A; lanes 1-4). RNA oligomers containing an m^{6}ACA sequence can only be cleaved by MazF after demethylation has occured[33]. In the absence of a PUF**a** target site, FTO and FTO-PUF**a** showed comparable m^{6}A demethylation activities in an RNA/DNA hybrid oligo (Fig. S2A), indicating that PUF**a** does not significantly interfere with the enzymatic activity of FTO when fused with it. Critically, at a concentration of 100 nM, at which both FTO and FTO-PUF**a** only weakly demethylated the m^{6}A in the RNA/DNA hybrid oligo, the demethylation activity of FTO-PUF**a** was significantly higher than that of FTO on an oligo bearing an m^{6}A 6 nucleotides (nt) away from the binding sequence of PUF**a** (Fig. 1A; lanes 5,6, Fig. 1B, Fig. S2B). FTO-PUF**a** also performed significantly better than FTO when the m^{6}A was located 2- and 10-nt away from the binding sequence of PUF**a** (Fig. S2C). When m^{6}A overlapped with the binding sequence of PUF**a** (5′-UGUAUAU(m^{6}A)-3′), no demethylation was observed (Fig. S2C). These results indicate that FTO-PUF**a** first binds to the PUF**a** binding site, triggering the demethylation of a nearby m^{6}A. Changing the linker between FTO and PUF**a** to $(GSS)_1$, $(GSS)_3$, or to a 39-amino acids linker (FXP)[34] did not significantly affect the demethylation of m^{6}A located 6-nt from the binding sequence of PUF**a** (Fig. S2D). It should be noted that the demethylation efficiency of FTO-PUF**a** for RNA containing the binding sequence reached a plateau at around 50%, even under higher concentrations of FTO-PUF**a** (Fig. S2E). One plausible reason is the stable RNA binding of PUF**a** to the target RNA sequence. The accessibility to the active center may also be restrained. Further engineering of FTO and PUFs from the viewpoint of the kinetics and the structure could improve the sequence-specific demethylation efficiency.

The sequence-specific demethylation activity of the FTO-PUF fusion proteins was further shown in the presence of competitive RNA fragments. Two kinds of FTO-PUF fusion proteins, FTO-PUF**a** and FTO-PUF**b** were prepared (Fig. 2A). PUF**b** was designed to target the RNA sequence 5′-UGGGGUUC-3′. Two different substrate RNAs, RNA[A^m] and RNA[B^m], in addition to a ~20-fold excessive amount of non-specific RNA fragment (246-nt) were mixed and incubated with each FTO-PUFs. RNA[A^m] and RNA[B^m] contained an m^{6}ACA sequence separated by 6 nt from the PUF**a** and PUF**b** binding sequences, respectively. In addition, RNA[A^m] and RNA[B^m] were 5′-labeled with the fluorescent labels FAM (ex. 488 nm) and TAMRA (ex. 532 nm), respectively (Fig. 2A). After the incubation of the mix of RNA[A^m] and RNA[B^m] with either FTO-PUF**a** or FTO-PUF**b**, the samples were treated with MazF and loaded onto a denaturing gel. Excitation of the gel at 488 nm revealed that MazF cleaved RNA[A^m] treated with FTO-PUF**a** but not with FTO-PUF**b** (Fig. 2B, upper); excitation at 532 nm showed cleaved RNA[B^m] bands only when the mix was treated with FTO-PUF**b** (Fig. 2B, lower). These results indicate that the FTO-PUFs efficiently discriminate their target sequences in a mixed population of RNAs. Moreover, FTO-PUFs could discriminate between their target RNAs even in the presence of extracted RNA from HeLa cells (Figs. 2C and S3A): RNA[A^m] and RNA[B^m] were specifically demethylated by FTO-PUF**a** and -PUF**b**, respectively. Next, gel mobility shift assay confirmed that FTO-PUF**a** bound only to RNA[A^m] and FTO-PUF**b** only to RNA[B^m] (Fig. S3B). These results demonstrate that the selective demethylation of substrate RNAs by PUF-fused FTO proteins depends on the selectivity of PUF domains.

We have shown that FTO-PUFs can be used *in vitro* for the demethylation of a methylated transcript. We next wondered whether PUFs could also be used to methylate a target RNA substrate. Therefore, we sought to use the same PUF-based

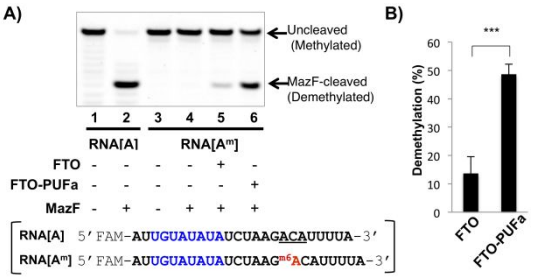

Figure 2 Fusion of the FTO demethylase with PUF RNA binding domain. (A) Demethylation activities of 100 nM of FTO (lane 5) and FTO-PUF**a** (lane 6) for the RNA substrate RNA[A^m] were examined by MazF cleavage. As shown in a parenthesis, RNA[A^m] contains an m^{6}ACA sequence and a PUF**a** binding sequence (blue letters). RNA[A], containing the same sequence as RNA[A^m] but non-methylated ACA (underlined), was used for the reference of MazF-cleaved band (lanes 1 and 2). RNA[A^m] was not cleaved by MazF (lanes 3 and 4). (B) The percentages of the demethylated substrate RNA by 100 nM of FTO or FTO-PUF**a** were calculated. Data are the mean ± S.D. The statistical analyses were performed using one-way ANOVA (***; p<0.001).

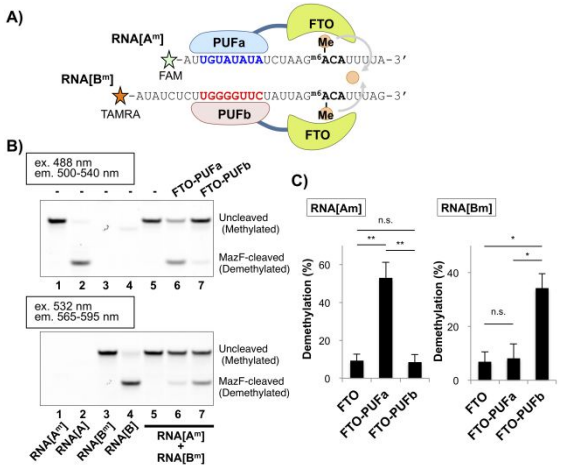

Figure 1 Sequence-specific demethylation by FTO-PUFs in the mixture of RNA substrates containing different PUF binding sites. (A) Design of FTO-PUF**a**, FTO-PUF**b**, and the substrate RNA containing their binding sites and m^{6}ACA sequences. The target sequences of PUF**a** and PUF**b** are shown in blue and red, respectively. 5′ terminal of RNA[A^m] and RNA[B^m] was labeled with FAM and TAMRA, respectively. (B) Demethylation activities of 100 nM of FTO-PUF**a** and FTO-PUF**b** in the mixture of two RNA probes, RNA[A^m] and RNA[B^m] (lanes 5-7; 50 nM each), in the presence of excess amount of in vitro transcribed non-specific RNA (246-nt, 100 nM). lanes 1-4; RNA controls, lane 5; no demethylase, lane 6; 100 nM FTO-PUF**a**, lane 7; 100 nM FTO-PUF**b**. The MazF–cleavage patterns of RNA[A^m] and RNA[B^m] after demethylation reaction were visualized by excitation with 488 nm (upper) and 532 nm (lower), respectively. (C) Demethylation activities of 100 nM of FTO, FTO-PUF**a**, or FTO-PUF**b** for RNA[A^m] (upper) and RNA[B^m] (lower) in the mixture of RNA[A^m] and RNA[B^m] (50 nM each) in the presence of 50 ng/μL total RNA extracted from HeLa cells. Data shown are the mean ± S.D. The statistical analyses were performed using one-way ANOVA (*; p<0.05, **; p<0.01, n.s.; not significant).

strategy to methylate target RNAs by fusing PUF proteins with the methyltransferase domain (MTD) of METTL14. The mRNA m^{6}A methylation is catalyzed by the METTL3/METTL14 heterodimer at the consensus sequence 5′-RRACH-3′[1]. Although both enzymes have MTDs, METTL3 is the catalytic core and METTL14 is believed to contribute to RNA substrate binding via its RNA binding groove and C-terminal RGG repeats[35-38]. We thus engineered the chimera MTD14d-PUF**a**, containing the MTase domain of METTL14 without the RGG repeats (aa 111-410) joined with the PUF domain (Fig. 3A). As a control we used the MTase domain of METTL14 with its native RGG domain (aa 111-456), thereafter denoted as MTD14. Strep-tagged METTL3 containing amino acids 255-580 (MTD3), together with His$_6$-tagged MTD14 or MTD14d-PUF**a** were expressed in *E. coli* and purified stepwise as a heterodimer, as described previously[33]. After methylation assay using these purified heterodimers, the samples were incubated with MazF and loaded onto a denaturing gel. The methylated levels were quantified using the ratio of uncleaved/cleaved substrates, since methylation of the RNA substrate inhibits the activity of MazF.

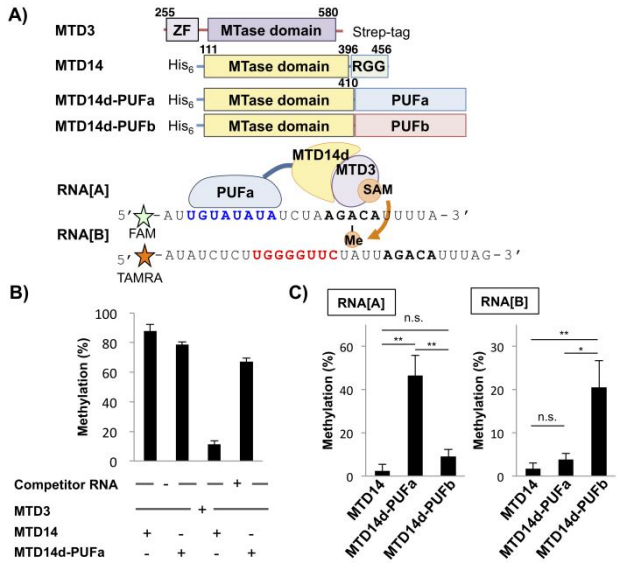

Figure 3 Construction of the methyltransferase-PUF fusion proteins. (A) Schematic representation of MTD3, MTD14 and MTD14d-PUFs and substrate RNAs. The target RNA sequences of PUF**a** and PUF**b** are colored in blue and red, respectively. The methylation target sequences (5′-RRACH-3′) are shown in bold letters. (B) Methylation activities of MTD3/MTD14 and MTD3/MTD14d-PUF**a** (100 nM) against RNA[A] (100 nM) in the absence or presence of non-specific RNA (246 nt, 700 nM). (C) Methylation activities of MTD3/MTD14, MTD3/MTD14d-PUF**a** or MTD3/MTD14d-PUF**b** (200 nM) against RNA[A] and RNA[B] (100 nM each) in the presence of 50 ng/μL of total RNA extracted from HeLa cells. Data shown are the mean ± S.D. The statistical analyses were performed using one-way ANOVA (*; p<0.05, **; p<0.01, n.s.; not significant) .

In the absence of competitive RNAs (Figs. 3B, S4A competitor (-)), both MTD3/MTD14 and MTD3/MTD14d-PUF**a** methylated about 80% of RNA[A], a substrate containing the PUF**a** binding sequence and a 5′-AGACA-3′ sequence 4 nucleotides downstream (compatible with the 5′-RRACH-3′ consensus and MazF-target sequence 5′-ACA-3′). In contrast, addition of an excess amount of non-specific RNAs (246-nt; 70-fold excess in nucleotides compared with RNA[A]) lowered the methylation level of RNA[A] by MTD3/MTD14 to <10%, while MTD3/MTD14d-PUF**a** still methylated about 70% of RNA[A] (Figs. 3B, S4A, competitor (+)).

While the MTDs are known to bind to RNA and provide some specificity to the target 5′-RRACH-3′ substrate, the RGG repeats of METTL14 likely contribute to RNA binding of the complex, albeit with low sequence specificity[35-38]. Indeed, the RNA[A] binding assay with MTD3/MTD14 showed MTD3/MTD14-dependent shifts in the absence of non-specific RNA; the shifts decreased when non-specific RNAs were added (Fig. S4B), suggesting that non-specific RNAs competed with RNA[A] for MTD3/MTD14 binding, resulting in decreased RNA[A] methylation. In contrast, RNA binding assays demonstrated that MTD14d-PUF**a** bound to RNA[A] regardless of the presence of non-specific RNAs (Fig. S4B), demonstrating the sequence specificity of MTD3/MTD14d-PUF**a** imparted by the RNA binding domain of PUF**a**.

Sequence specificity of MTD3/MTD14d-PUF**a** was further demonstrated in a mixture of substrate RNAs with different PUF-target sequences. A second METTL14-PUFs chimera, binding to a different RNA sequence substrate (RNA[B]), was engineered and named MTD14d-PUF**b**. RNA[A] and RNA[B] both included a 5′-AGACA-3′ sequence 4 nucleotides downstream of their respective PUF binding sites (PUF**a** or PUF**b**) and were labeled with the fluorescent tags FAM and TAMRA, respectively (Fig. 3A). As before, MTD14d-PUF**a** or MTD14d-PUF**b** were co-expressed with MTD3 in *E. coli* and purified as a complex. MTD3/MTD14d-PUF**a** and MTD3/MTD14d-PUF**b** were then incubated with equimolar amounts (100 nM each) of RNA[A] and RNA[B] in the presence of an excess amount of competitor RNAs (246-nt, 300 nM); their methylation activities were evaluated using the MazF-cleavage assay. Excitation of the gel at 488 nm revealed that the intensity of uncleaved RNA[A] increased in correlation with the concentration of MTD3/MTD14d-PUF**a** but not -PUF**b** (Fig. S5A, upper). Similarly, at 532 nm, the intensity of uncleaved RNA[B] increased with the concentration of MTD3/MTD14d-PUF**b** but not that of MTD3/MTD14d-PUF**a** (Fig. S5A, lower). These results demonstrate the specificity of MTD3/MTD14d-PUF**a** and -PUF**b**. The specificity of these chimeras was further confirmed even in the presence of total RNA extracted from HeLa cells (Figs. 3C, S5B), demonstrating the feasibility of customizable PUF-fused METTL14 MTD chimera for targeted mRNA m^{6}A methylation.

In this study, we have engineered m^{6}A regulatory enzymes based on modular PUFs fused with FTO and METTL14. FTO-PUFs demethylated m^{6}A close to the binding site of the PUF RNA binding domain, while MTD3/MTD14d-PUFs methylated the N^6 adenosine in a 5′-RRACH-3′ consensus sequence close to the binding site of PUFs. Sequence-specific (de)methylation was demonstrated *in vitro* even in the presence of an excess amount of non-specific RNA fragments derived from mammalian cells, strongly suggesting these chimeras could be used in cell cultures or even *in vivo*. Although further

examinations are needed, these results provide a proof-of-principle that the strategy to fuse m^{6}A-regulatory enzymes with the programmable RNA binding protein PUF is a promising way for site-specific control of RNA methylation, not only at the transcript level but also at the level of a single m^{6}A site within a given transcript. Very recently, sequence-specific regulation of RNA methylation and demethylation was reported using a CRISPR-dCas9-PAMer-sgRNA system fused with demethylases[39, 40] and MTases[39]. Compared with the Cas-gRNA complexes, the molecular size of PUFs is much smaller, simplifying the construction of expression vectors encoding chimeric demethylases or methyltransferases. Critically, the small molecular size of PUFs allowed RNA (de)methylation in the immediate vicinity of the binding site, for which PUFs were designed. Our study shows that customizable RNA binding proteins based on PUFs are a promising alternative to Cas9 and Cas13 systems. Indeed, PUFs are modular and intrinsically sequence-specific, and, unlike Cas, do not require guide RNAs.

This work was supported by JST/CREST (JPMJCR14W3 to M.I.), by JSPS/KAKENHI (16H03281, 19H02850 to M.I.), and by Kenzo Suzuki Memorial Foundation (to M.I.). We thank Dr. Jean-Michel Fustin for his valuable comments on the draft.

Conflicts of interest

There are no conflicts to declare.

Notes and references

1. J. Liu, Y. Yue, D. Han, X. Wang, Y. Fu, L. Zhang, G. Jia, M. Yu, Z. Lu, X. Deng, Q. Dai, W. Chen and C. He, *Nat Chem Biol*, 2014, **10**, 93-95.
2. G. F. Jia, Y. Fu, X. Zhao, Q. Dai, G. Q. Zheng, Y. Yang, C. Q. Yi, T. Lindahl, T. Pan, Y. G. Yang and C. He, *Nat Chem Biol*, 2011, **7**, 885-887.
3. G. Q. Zheng, J. A. Dahl, Y. M. Niu, P. Fedorcsak, C. M. Huang, C. J. Li, C. B. Vagbo, Y. Shi, W. L. Wang, S. H. Song, Z. K. Lu, R. P. G. Bosmans, Q. Dai, Y. J. Hao, X. Yang, W. M. Zhao, W. M. Tong, X. J. Wang, F. Bogdan, K. Furu, Y. Fu, G. F. Jia, X. Zhao, J. Liu, H. E. Krokan, A. Klungland, Y. G. Yang and C. He, *Mol Cell*, 2013, **49**, 18-29.
4. P. J. Batista, B. Molinie, J. Wang, K. Qu, J. Zhang, L. Li, D. M. Bouley, E. Lujan, B. Haddad, K. Daneshvar, A. C. Carter, R. A. Flynn, C. Zhou, K. S. Lim, P. Dedon, M. Wernig, A. C. Mullen, Y. Xing, C. C. Giallourakis and H. Y. Chang, *Cell Stem Cell*, 2014, **15**, 707-719.
5. Y. Wang, Y. Li, J. I. Toth, M. D. Petroski, Z. Zhang and J. C. Zhao, *Nat Cell Biol*, 2014, **16**, 191-198.
6. D. Dai, H. Wang, L. Zhu, H. Jin and X. Wang, *Cell Death Dis*, 2018, **9**, 124.
7. S. Lin, J. Choe, P. Du, R. Triboulet and R. I. Gregory, *Mol Cell*, 2016, **62**, 335-345.
8. J. M. Fustin, M. Doi, Y. Yamaguchi, H. Hida, S. Nishimura, M. Yoshida, T. Isagawa, M. S. Morioka, H. Kakeya, I. Manabe and H. Okamura, *Cell*, 2013, **155**, 793-806.
9. E. M. Kennedy, D. G. Courtney, K. Tsai and B. R. Cullen, *J Virol*, 2017, **91**. e02263.
10. Y. Pei and M. Lu, *Cell Mol Life Sci*, 2019, 10.1007/s00018-019-03252-9.
11. Z. Abil and H. M. Zhao, *Mol Biosyst*, 2015, **11**, 2658-2665.
12. S. Rauch, E. He, M. Srienc, H. Q. Zhou, Z. J. Zhang and B. C. Dickinson, *Cell*, 2019, **178**, 122-134.
13. X. Wang, P. D. Zamore and T. M. Hall, *Mol Cell*, 2001, **7**, 855-865.
14. T. A. Edwards, S. E. Pyle, R. P. Wharton and A. K. Aggarwal, *Cell*, 2001, **105**, 281-289.
15. A. Filipovska, M. F. Razif, K. K. Nygard and O. Rackham, *Nat Chem Biol*, 2011, **7**, 425-427.
16. S. Dong, Y. Wang, C. Cassidy-Amstutz, G. Lu, R. Bigler, M. R. Jezyk, C. Li, T. M. Hall and Z. Wang, *J Biol Chem*, 2011, **286**, 26732-26742.
17. X. Wang, J. McLachlan, P. D. Zamore and T. M. Hall, *Cell*, 2002, **110**, 501-512.
18. C. G. Cheong and T. M. Hall, *Proc Natl Acad Sci U S A*, 2006, **103**, 13635-13639.
19. Z. T. Campbell, C. T. Valley and M. Wickens, *Nat Struct Mol Biol*, 2014, **21**, 732-738.
20. K. Shinoda, S. Tsuji, S. Futaki and M. Imanishi, *Chembiochem*, 2018, **19**, 171-176.
21. Y. Y. Zhao, M. W. Mao, W. J. Zhang, J. Wang, H. T. Li, Y. Yang, Z. Wang and J. W. Wu, *Nucleic Acids Res*, 2018, **46**, 4771-4782.
22. K. P. Adamala, D. A. Martin-Alarcon and E. S. Boyden, *Proc Natl Acad Sci U S A*, 2016, **113**, E2579-2588.
23. Y. Wang, C. G. Cheong, T. M. Hall and Z. Wang, *Nat Methods*, 2009, **6**, 825-830.
24. J. Cao, M. Arha, C. Sudrik, A. Mukherjee, X. Wu and R. S. Kane, *Nucleic Acids Res*, 2015, **43**, 4353-4362.
25. A. Cooke, A. Prigge, L. Opperman and M. Wickens, *Proc Natl Acad Sci U S A*, 2011, **108**, 15870-15875.
26. Z. Abil, C. A. Denard and H. Zhao, *J Biol Eng*, 2014, **8**, 7.
27. R. Choudhury, Y. S. Tsai, D. Dominguez, Y. Wang and Z. Wang, *Nat Commun*, 2012, **3**, 1147.
28. H. Yoshimura, A. Inaguma, T. Yamada and T. Ozawa, *ACS Chem Biol*, 2012, **7**, 999-1005.
29. T. Yamada, H. Yoshimura, A. Inaguma and T. Ozawa, *Anal Chem*, 2011, **83**, 5708-5714.
30. T. Ozawa and Y. Umezawa, *Methods Mol BIol*, 2011, **714**, 175-188.
31. T. Ozawa, Y. Natori, M. Sato and Y. Umezawa, *Nat Methods*, 2007, **4**, 413-419.
32. T. Yamada, H. Yoshimura, R. Shimada, M. Hattori, M. Eguchi, T. K. Fujiwara, A. Kusumi and T. Ozawa, *Sci Rep*, 2016, **6**, 38910.
33. M. Imanishi, S. Tsuji, A. Suda and S. Futaki, *Chem Commun (Camb)*, 2017, **53**, 12930-12933.
34. V. Schellenberger, C. W. Wang, N. C. Geething, B. J. Spink, A. Campbell, W. To, M. D. Scholle, Y. Yin, Y. Yao, O. Bogin, J. L. Cleland, J. Silverman and W. P. Stemmer, *Nat Biotechnol*, 2009, **27**, 1186-1190.
35. P. Wang, K. A. Doxtader and Y. Nam, *Mol Cell*, 2016, **63**, 306-317.
36. P. Sledz and M. Jinek, *Elife*, 2016, **5**, e18434.
37. X. Wang, J. Feng, Y. Xue, Z. Guan, D. Zhang, Z. Liu, Z. Gong, Q. Wang, J. Huang, C. Tang, T. Zou and P. Yin, *Nature*, 2016, **534**, 575-578.
38. E. Scholler, F. Weichmann, T. Treiber, S. Ringle, N. Treiber, A. Flatley, R. Feederle, A. Bruckmann and G. Meister, *RNA*, 2018, **24**, 499-512.
39. X. M. Liu, J. Zhou, Y. Mao, Q. Ji and S. B. Qian, *Nat Chem Biol*, 2019, **15**, 865-871.
40. K. Rau, L. Roesner and A. Rentmeister, *RNA*, 2019, **25**, 1311-1323.